Propagation and Termination Kinetics of Cross-Linking Photopolymerizations Studied Using Electron Paramagnetic Resonance Spectroscopy in Conjunction with Near IR Spectroscopy

Kathryn A. Berchtold,[†,‡] Theodore W. Randolph,[†] and Christopher N. Bowman*[,†,§]

Department of Chemical and Biological Engineering, University of Colorado, Boulder, Colorado 80309-0424, Materials Science & Technology Division, MST-7, Los Alamos National Laboratory, Mail Stop E-549, Los Alamos, New Mexico 87545, and Department of Restorative Dentistry, University of Colorado Health Sciences Center, Denver, Colorado 80045-0508

Received March 28, 2005; Revised Manuscript Received June 11, 2005

ABSTRACT: The use of electron paramagnetic resonance (EPR) in conjunction with Fourier transform near infrared (FT-NIR) spectroscopy to address the complexities associated with the accurate measurement and evaluation of cross-linking polymerization kinetics over the entire conversion range is explored. Experimental protocols are developed providing a more complete picture of the mechanistic and kinetic underpinnings of these radical polymerizations, accessing information that is otherwise unavailable to these techniques individually. The kinetics of two multimethacrylate polymerization systems, one forming a rubbery and the other a glassy polymer network, are compared and contrasted revealing numerous differences in their attributes as characterized by this experimental combination. Steady-state and unsteady-state radical concentration profiles, propagating radical environments during polymerization, and persistent radical populations are explored and utilized to evaluate the underlying propagation and termination kinetics. Subsequently, kinetic parameters obtained with EPR and EPR/FT-NIR are compared with those obtained independently from FT-NIR, enabling evaluation of the assumptions that underlie each technique.

Introduction

Over the years, many techniques have been used to probe the kinetics of cross-linking photopolymerizations. Tools such as differential scanning calorimetry (DSC) and real-time infrared spectroscopy are commonly used to examine the kinetics of such systems. These methods enable monitoring of the decay of reactive functionalities as a function of polymerization time. The kinetics are also strongly dependent on the radical concentration, which is not directly measured by the aforementioned techniques. Correspondingly, the environment and the structure of the radical species are also not available for analysis with these methods. Electron paramagnetic resonance (EPR) spectroscopy is a powerful technique, which provides a means for direct observation of the radical populations formed during polymerization.[1] The ability to monitor the radical species directly provides insight into the kinetics of these reactions as well as into the long-term mechanical properties of the resulting networks. The termination process of the radical species is observed and the extent of radical trapping in the network quantified. In this work, EPR spectroscopy has been used in conjunction with Fourier transform near-infrared (FT-NIR) spectroscopy to obtain information about the radical populations during photopolymerization of two multimethacrylate polymerization systems, one forming a rubbery polymer network and the other a glassy network. Specifically, steady-state radical concentration profiles, unsteady-state radical concentration profiles, environments of the propagating radicals throughout the majority of the polymerization, and persistent radical populations are explored. That information is subsequently used for evaluation of propagation and termination kinetics over the entire conversion range of the polymerization. Kinetic constants are evaluated both with and without incorporation of persistent radical population information, and the impact of those populations is assessed. Additionally, kinetic parameters obtained using EPR and EPR/FT-NIR are compared with those obtained independently from FT-NIR. This comparison allows for evaluation of the assumptions that underlie those techniques. Furthermore, the validity of using radical concentration information for a *single* steady-state polymerization conducted in the cavity of the EPR in conjunction with the pseudo-steady-state assumption to calculate the termination kinetics as a function of conversion over the entire conversion range is evaluated.

Background

Kamachi[2] and Yamada et al.[3] have reviewed much of the work that has been done relating to EPR spectroscopy of radical polymerizations. To date, much of the work that has been done involving characterization of polymerization kinetics with EPR has been limited to linearly polymerizing monomers and polymerizations forming soluble polymer,[2−16] with the majority of the work focused on methyl methacrylate and styrene polymerizations. Investigations that probe the propagation and/or termination kinetics of multivinyl cross-linking polymerizations with EPR are few.[7,17−20] The works that have determined the radical structures underlying the observed spectra provide the foundation for using this technique as a tool for obtaining kinetic information. For methacrylate polymerizations, such as those under evaluation in this work, the positive

* To whom correspondence should be addressed. E-mail: Christopher.Bowman@colorado.edu. Fax: (303) 492-4341.
[†] Department of Chemical and Biological Engineering, University of Colorado.
[‡] Los Alamos National Laboratory.
[§] University of Colorado Health Sciences Center.

10.1021/ma0506482 CCC: $30.25
Published on Web 07/15/2005

identification and subsequent assignment of the typically observed 13- and 9-line radical spectra and the environment(s) in which those radical species exist were scrutinized for quite some time[21−31] before their current, accepted explanations were reached.[3,31] In addition, the methods used for obtaining radical concentrations as a function of polymerization time have also advanced quite significantly over the years. Initially, samples were frozen so that radicals could be stabilized for a period of time long enough to collect a spectrum.[2] With advances in cavity design, spectrometer sensitivity, and collection techniques, spectra are now collected in situ during polymerization.[3] Additionally, the development of collection techniques, specifically the use of static-field collection, has been particularly useful for increasing the attainable temporal resolution. This technique, which involves monitoring a single magnetic field value, has been used by a number of authors to capture radical concentrations early in the polymerization when the change in concentration is quite rapid.[5,7,17,32−34] Furthermore, Chang et al. have used this technique to monitor the thermal, emulsion polymerization of MMA throughout the polymerization with a temporal resolution of 2.6 s.[33,34] This work takes advantage of the aforementioned advances and builds upon prior research in the area. To our knowledge, these technique advances have not yet been utilized to evaluate the kinetics of polymerizations that occur on time scales of less than hundreds of seconds. This work uses the time advantages of the static-field technique to collect kinetic data with millisecond temporal resolution. Collections at this resolution make it possible to evaluate polymerizations that occur on much faster time scales over their entire conversion range as well as termination behavior that occurs in the first second(s) following the removal of the initiation reaction, making it possible to calculate the short-time termination kinetics.

The value of quantifying radical concentrations during polymerization to the evaluation of the underlying propagation and termination kinetics is clear. However, one can also hypothesize that experiments that seek to quantify the portion of the total radical concentration that actively participates in those reactions are equally important, especially in polymerizations that form cross-linked networks. The existence of such "trapped" or persistent populations is an accepted phenomenon.[1,24,35−38] Understanding the evolution of such a population as the polymerization progresses is important to the complete assessment of the polymerization kinetics of these complex systems. Evaluation and quantification of the population of radicals that remains in the network post polymerization is also of significant value, as that population will have an impact on the long-term stability of the polymer product. If such a radical population remains, the potential exists for the "final" mechanical, chemical, and material properties of the polymer to evolve over time. Such a system could be adversely affected by a variety of factors such as thermal cycling, weathering, and mechanical stress. Residual radicals react further with unreacted double bonds and oxygen leading to negative property changes, e.g., stress development, brittleness, and peroxide formation, over time. The trapping of radicals in glassy, cross-linked polymer networks and their subsequent decay via temperature cycling and time have been studied using EPR by several authors.[32,39,40] This type of information, in conjunction with the conversion and rate information obtainable from other techniques, provides a more complete picture of the polymerization.

Materials

The monomers used as received in this study were poly(ethylene glycol) (600) dimethacrylate (PEG(600)DMA, Sartomer Co., Exton, PA), tri(ethylene glycol) dimethacrylate (TEGDMA, Polysciences Inc., Warrington, PA), and 2,2-bis-[4(2-hydroxy-3-methacryloxy-propyloxy)-phenyl]propane (bis-GMA, Cook Composites and Polymers, Kansas City, MO). The numeric notation in the PEG(600) monomer refers to the average molecular weight of the ethylene glycol chain of the macromer. Polymerizations were performed using 0.1 wt % of the ultraviolet initiator 2,2-dimethoxy-2-phenylacetophenone (DMPA, Ciba Geigy, Hawthorne, NY). α,α′-Diphenyl-1-picrylhydrazyl (Aldrich, Milwaukee, WI) was the stable free radical used for concentration calibrations. Hydrogenated TEGDMA was used as the solvent for the concentration calibration standards.

Hydrogenated TEGDMA Synthesis. An unreactive version of the monomer TEGDMA was prepared via hydrogenation[41,42] of the reactive species. Palladium catalyst (1 g, 3% Pd on activated carbon) was added to a TEGDMA/ethyl acetate solution (10 g/100 mL). Hydrogen gas was bubbled through the stirred suspension at ambient conditions until the reaction was complete, 18−36 h. The catalyst was removed from the product by filtration through Celite, and the solvent was removed via evaporation under reduced pressure. IR and NMR were used to verify complete reduction of the methacrylate carbon−carbon double bond without additional alterations to the monomer structure.

Methods

Irradiation Source. An UV light source (Ultracure 100SS 100-W high-pressure mercury vapor short-arc lamp, EXFO, Mississaugua, Ontario, Canada) equipped with a liquid light guide was used to irradiate the monomer/initiator mixtures in the sample chambers of the FTIR and EPR spectrometers. The spectral output of the lamp was controlled with a band-pass filter (320−390 nm, peak 365 nm, EXFO, Mississaugua, Ontario, Canada). The incident light intensity was controlled using the internal aperture of the UV light source and measured with a UV radiometer with a silicone photoelectric sensor (Cole-Parmer Series 9811 Radiometer, Vernon Hills, IL). All polymerizations were performed using an irradiation intensity of 5 mW/cm^2. The molar absorptivity of the photoinitiator, DMPA, at the peak initiating wavelength, 365 nm, is 150 L/(mol·cm).

FT-NIR. Real-time FT-NIR spectroscopy has been used to monitor the polymerization kinetics. A horizontal transmission accessory (HTA) was designed to enable mounting of samples in a horizontal orientation for FTIR measurements.[19,43] This orientation allows measurements on thick and/or low viscosity films without the flow problems inherent to the standard vertical arrangement. This accessory also facilitates irradiation of samples from a near-normal incidence without interfering with the IR source.

Temperature control was achieved using a temperature control device designed using Peltier technology (Ferro Tec-SuperTEC single stage coolers, Manchester, NH) and constructed for use in conjunction with the HTA. A FTIR spectrophotometer (Nicolet Model 760 Magna Series II FTIR, Nicolet, Madison, WI) was used to monitor the polymerization kinetics. An InGaAs-XT KBr detector-beam splitter combination was used in conjunction with the rapid-scan feature of the spectrometer to obtain temporal resolutions (∼30 ms) sufficient for monitoring these polymerizations.

NIR samples were prepared by injecting monomer into molds constructed using glass slides with 1.0-mm silicone sheeting as spacer material. The sample thickness outlined above was chosen for a number of reasons: (1) For the materials studied, 1 mm is an appropriate thickness to get strong, unsaturated FT-NIR spectra throughout the conversion

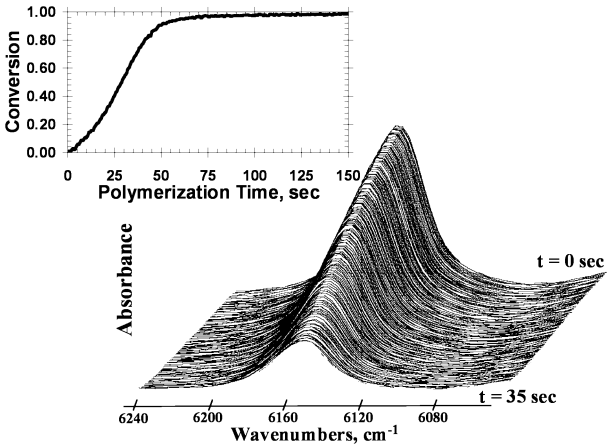

Figure 1. Illustration of the decay in the vinyl CH_2 absorbance as a function of polymerization time for PEG(600)DMA. The area of the NIR overtone peak at ca. 6160 cm^{-1} can be directly translated into conversion vs time data (inset plot). Polymerization conditions: light Intensity, 5 mW/cm^2; photoinitiator (DMPA) concentration, 0.1 wt %.

of monomer to polymer. (2) At the initiator concentrations studied, 1 mm is an appropriate thickness to minimize the initiating light attenuation through the sample, i.e., maintaining an approximately constant initiation rate as a function of sample thickness, while maximizing the obtainable EPR signal. (3) 1 mm matches the thickness of the samples prepared for analysis using EPR, readily allowing for comparisons between the FT-NIR and EPR rates and kinetics and enabling correlation between EPR reaction times and monomer conversion when EPR and FT-NIR experiments are run under the same conditions. (4) Additionally, this sample thickness is also appropriate for dynamic mechanical analysis (DMA), solubility, swelling, extraction, and degradation studies, thus allowing material property studies on the same samples used for kinetic studies when desired. FT-NIR spectra are analyzed to ascertain the change in the vinyl CH_2 absorbance as a function of polymerization time (Figure 1). The area of the CH_2 stretch first overtone peak at ca. 6160 cm^{-1} was used as a measure of double-bond conversion.

FTIR Analysis. Double-bond conversion as a function of time is measured using FT-NIR. Correspondingly, the polymerization rate is obtained from the derivative of the conversion vs time information (Figure 1 inset). Kinetic parameters, a function of conversion, are also available using FT-NIR. In this work termination and propagation kinetic constants obtained from FT-NIR are compared to those calculated using a combination of the FT-NIR and EPR techniques.

Termination and propagation kinetic parameters are obtained from FT-NIR via unsteady-state experiments. In these experiments the initiating light source is extinguished during photopolymerization, and the polymerization is monitored "in the dark." In the absence of initiation (i.e., after the light is extinguished), the kinetics, assuming a bimolecular chain length independent termination mechanism, are described by the following species balances on the radicals and double bonds present in the system

$$\frac{d[\mathrm{R}\bullet]}{dt} = -2kt[\mathrm{R}\bullet]^2 \tag{1}$$

$$\frac{d[\mathrm{M}]}{dt} = -k_\mathrm{p}[\mathrm{M}][\mathrm{R}\bullet] \tag{2}$$

where k_t and k_p are the kinetic constants for termination and propagation, [R•] and [M] are radical and double-bond concentrations, and t is time. An expression for [R•] as a function of time is obtained via integration of the radical population balance, eq 1, where the lower integration limit of [R•] at t = 0 in the dark is $[\mathrm{R}\bullet]_0$ or R_{p0}/k_p·[M]. The resultant radical

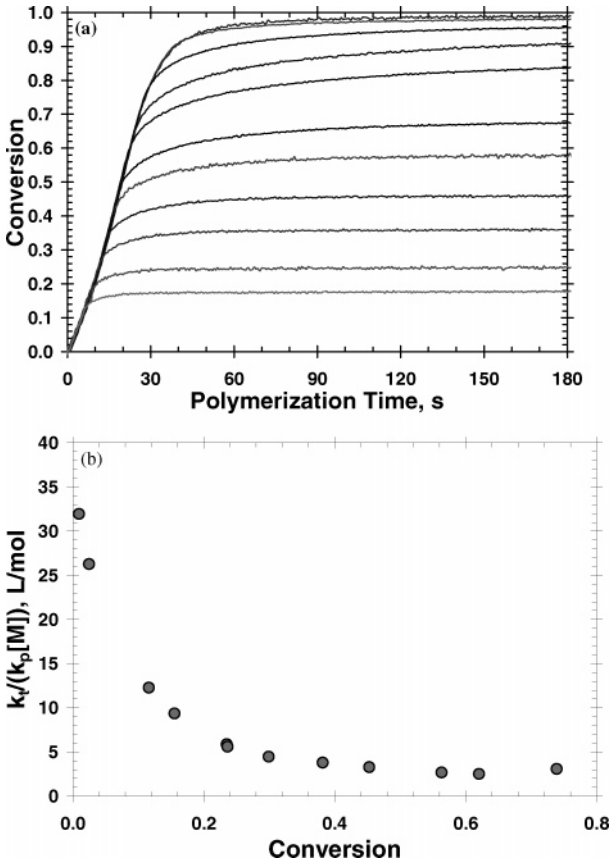

Figure 2. "In the dark" experiments for PEG(600)DMA. Conversion vs time is presented in (a). Each line represents a single run where the light was extinguished at a specific time/conversion and then monitored "in the dark." The kinetic constant ratio, k_t/k_p[M], as a function of conversion determined from the experiments in (a) are presented in (b). The plateau value is R, the reaction diffusion constant. Polymerization conditions: initiator (DMPA) concentration, 0.1 wt %; light intensity, 5 mW/cm^2; temperature, 25 °C.

concentration expression, eq 3, is then substituted into the balance on double bonds, eq 2

$$[\mathrm{R}\bullet] = \frac{R_{p0}/(k_\mathrm{p}[\mathrm{M}])}{2R_{p0}R(t - t_0) + 1} \tag{3}$$

where R is the ratio of kinetic constants k_t/k_p[M]. The resulting expression is then simplified, and the ratio of kinetic constants, R, is obtained directly from the following result[44]

$$\Delta[\mathrm{M}] = \frac{1}{2R}\ln(2RR_{p0}t + 1) \tag{4}$$

where R_{p0} is the polymerization rate at t = 0 in the dark, Δ[M] is the change in double-bond concentration, and t is the time for which the change in double-bond concentration is monitored in the absence of initiation.

An example of the experimental conversion vs time profiles for a complete series of unsteady-state experiments and the kinetic information available from those experiments is presented in Figure 2.

To decouple the kinetic constants, the value of R is combined with the steady-state kinetic expression (eq 5), just prior to the extinction of the light[44]

$$R_\mathrm{p} = \frac{k_\mathrm{p}}{k_\mathrm{t}^{(1/2)}}[\mathrm{M}]\left(\frac{R_\mathrm{i}}{2}\right)^{(1/2)} \tag{5}$$

In this expression, R_i is the initiation rate. The initiation rate

for each polymerization was calculated[45] from the following expression

$$R_i = 2\phi I_{abs} = 2\phi((2.303\epsilon I_{inc}\lambda[Ab]/N_{Av}hc)) \quad (6)$$

where ϕ is the initiator efficiency (assumed one for all calculations), I_{abs} the quantity of light absorbed, ϵ the initiator's molar absorptivity at λ, the wavelength of initiation, I_{inc} the incident light intensity in units of power/area, [Ab] the initiator concentration, N_{Av} Avogadro's number, h Planck's constant, and c the velocity of light.

It is important to note that the determination of the kinetic parameters using FTIR alone utilizes both a pseudo-steady-state assumption applied to the radical concentration and implicit knowledge of the initiation rate. These assumptions are not required for kinetic parameter determination using EPR and FT-NIR in combination. Thus, the validity of those assumptions is also evaluated by comparing the kinetic parameters obtained with both techniques.

EPR Spectroscopy Measurements. A Bruker ESP300E EPR spectrometer (Bruker Analytik GmbH, Rheinstetten/Karlsruhe, Germany) operating in the X-band was used to study the radical concentration profiles during polymerization. A TE_{102} cavity, 100-kHz field modulation, and 2-G_{pp} modulation amplitude were used for all experiments.

Sample Preparation. Nitrogen was bubbled through all monomer/initiator mixtures for 10 min prior to preparing samples for EPR analysis. Polymerization samples were sealed in 1 mm inside diameter (i.d.) capillary tubes under a nitrogen purge using a fill height of 25 mm. Capillary tubes containing samples were then placed in a thick-walled quartz EPR sample tube (Wilmad precision quartz model 700-PQ-7 sample tube, 1.40 mm wall thickness, 2.16 mm i.d., Wilmad Glass, Buena, NJ) and then into a TE_{102} cavity for analysis. A double-walled quartz dewar insert (Wilmad Suprasil Quartz dewar insert, model 821-F-Q, Wilmad Glass, Buena, NJ) was inserted in the cavity during all experimentation. The purpose of the dewar insert was 2-fold. It was required for its standard purpose, namely, temperature control of the cavity. Additionally, its presence, in combination with the thick-walled quartz EPR tube, was necessary to adjust the sensitivity of the cavity so that a signal could be recorded from the small sample sizes present in the 1-mm capillary tubes. A steady nitrogen flow was maintained through the microwave cavity during all experimentation. Polymerizations were carried out while the sample was inside the EPR cavity. This method allowed the presence of radicals to be monitored during the polymerization. All experiments were performed at 25 °C.

Microwave Power Selection. The signal acquired from the crystal detector of a reflection cavity EPR spectrometer is proportional to the square root of the microwave power (MWP) incident on the sample cavity in the absence of saturation.[46] Thus, an analysis of the MWP saturation characteristics of the radicals to be evaluated is necessary. MWP saturation plots for several of those systems were generated to determine the optimum MWP at which to run quantitative kinetic experiments. This determination involves reaching a compromise between maximizing sensitivity, i.e., obtaining signal at the lowest possible radical concentrations, and minimizing the necessary saturation correction. The saturation behavior of the persistent methacrylate propagating radical population in polymerized TEGDMA is presented in Figure 3. The sample used for this determination was photopolymerized to 72% conversion as determined by NIR spectroscopy. The signal intensity is quantified via the area under the absorbance curve of the evaluated sample at the experimental conditions, or the double integral of the typically presented first derivative spectrum.

Unfortunately, at the low powers necessary to avoid saturation, <0.6 mW, a satisfactory signal is not obtained at short irradiation times, i.e., low conversion, during photopolymerization. Experiments at a MWP of 2 mW (20 dB attenuation) produced satisfactory signal at low conversions (low radical concentrations) while necessitating only a small saturation correction. The saturation correction factor, S, was calculated by a ratio of the signal intensity expected in the absence of saturation, I_{unsatd}, to the experimentally measured signal, I_{expt}, at the desired MWP. I_{unsatd} is calculated via extrapolation from the linear fit obtained at low MWP as depicted in Figure 3. S for this system at 2 mW is 1.4.

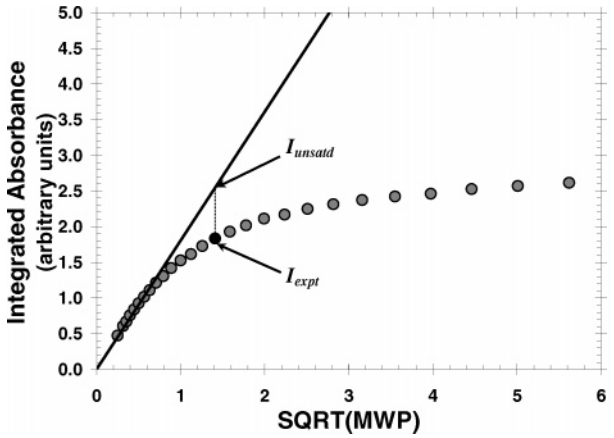

Figure 3. MWP saturation characteristics of the persistent methacrylate-propagating radical population in photopolymerized TEGDMA at 72% conversion. The MWP chosen for EPR experimentation, 2 mW, is highlighted (●). Polymerization conditions: light intensity, 5 mW/cm^2; initiator concentration, 0.1 wt %. EPR operation conditions: microwave frequency, 9.4 GHz; modulation frequency, 100 kHz; modulation amplitude, 2.0 G_{pp}; receiver gain, 4×10^4; temperature, 25 °C.

EPR measurement sensitivity is a strong function of the sample's dielectric loss. The dielectric characteristics of monomer/polymer systems are both a function of the system polymerized and the extent of conversion of a given polymerization sample. Thus, the saturation characteristics of the methacrylate propagating radical in different "solvents" were also evaluated to assess variations in saturation behavior as a function of conversion for a given monomer/polymer system and as a function of the monomer system polymerized.

The results of this saturation behavior characterization are well represented by the saturation behavior of the persistent methacrylate-propagating radical population in polymerized TEGDMA at low conversion, ~48%, and in polymerized 2,2-bis[4(2-hydroxy-3-methacryloxy-propyloxy)-phenyl]propane (bisGMA) (Structure I), ~34% conversion. BisGMA was chosen for evaluation as it represents a monomer system with a dramatically different chemical makeup than TEGDMA while still having the same propagating radical species. S for the lower conversion TEGDMA and bisGMA solvent systems presented here at a MWP of 2 mW is 1.2 and 1.3, respectively. These results, in addition to similar analyses on a number of other polymerization systems, indicate that measurable saturation corrections at 2 mW are consistently between 1.2 and 1.4 for the methacrylate-propagating radical present in a range of monomer/polymer solvents.

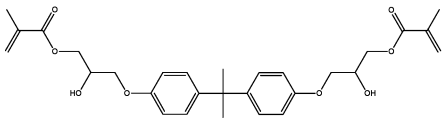

(I)

A measure of the change in saturation behavior is not readily attainable as a function of the entire conversion range for any given system. Extrapolation of the data available at conditions where persistent radical populations are present, and thus saturation measurements possible, would only lead to an increased uncertainty in the final concentration measurements. Therefore, the average measured saturation correction over a range of polymerization systems and conversions, $S = 1.3$, was used for all calculations.

Concentration Calibration. Conversion of the measured signal intensity to radical concentration is necessary for kinetic

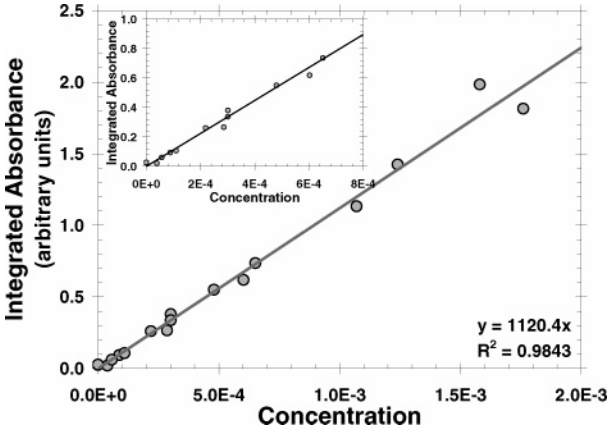

Figure 4. Concentration calibrations obtained using DPPH in hydrogenated TEGDMA. The low-concentration region is expanded in the inset plot for easier evaluation. Operation conditions: microwave frequency, 9.39 GHz; modulation frequency, 100 kHz; modulation amplitude, 2.0 G_{pp}; temperature, 25 °C.

parameter analysis and quantitative comparisons with previously conducted research. α,α′-diphenyl-1-picrylhydrazyl (DPPH), was used as the stable free radical for concentration calibration standardization. It is desirable to prepare standard samples in the same solvent as the samples in need of calibration. However, DPPH reacts in the presence of methacrylate species. Correspondingly, monomer cannot be used as the solvent. The appropriate monomer substitute is a nonreactive, i.e., hydrogenated, version of the monomer. Thus, the hydrogenated version of TEGDMA was synthesized for that purpose.

Standards were prepared and evaluated using the same sample geometry, volume, preparation technique, and acquisition conditions as the polymerization samples. The resultant relationship between signal intensity and radical concentration is presented in Figure 4. This relationship deviates significantly from one devised using DPPH in benzene illustrating the importance of choosing a solvent that resembles the system to be evaluated.

Polymerization Characterization. Monitoring the entire radical spectra as a function of time is the most straightforward way of accumulating radical concentration profiles and monitoring spectral changes during polymerization. Experiments were performed on stable radicals to determine the rate at which data could be acquired without distortion of the results. A temporal resolution of ~7 s was the result. This time resolution is quite poor when studying polymerizations that occur in seconds or even those that occur in tens of seconds. This temporal resolution also becomes a major limitation when examining termination kinetics, i.e., examining the radical population decay upon extinction of the initiating irradiation source. In such scenarios at low conversions, the visible radical population quickly drops to low and often undetectable levels, generally before even a single data point is collected.

This work has employed data acquisition at a static magnetic field value to enhance the time response of the system. Other authors have used similar techniques to monitor polymerization kinetics but, to this point, only for reactions occurring on much longer time scales.[5,7,17,32−34] The field value at the center line peak of the main methacrylate propagating radical spectra[2] was chosen. The radical spectra present during the polymerization of the PEG(600)DMA and TEGDMA systems exhibit minimal changes during the course of the polymerization, and thus the application of this technique is straightforward. Studies were done to determine the correlation between peak height and spectral area for these polymerizations. A linear relationship was obtained, validating the use of peak height for radical concentration measurements.

In the case of the system that forms a rubbery polymerization network, PEG(600)DMA, the 13-line spectrum associated with the methacrylate propagating radical in a liquidlike

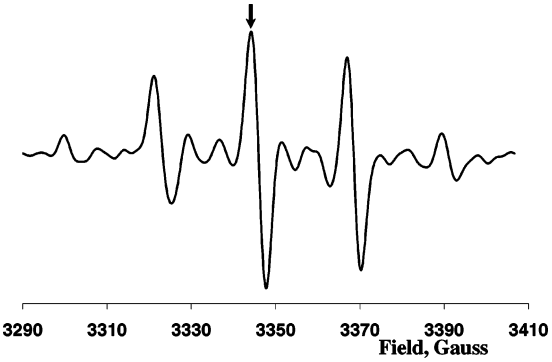

Figure 5. Typical 13-line methacrylate-propagating radical EPR spectra acquired during the polymerization of PEG(600)-DMA. Arrow indicates the field position used during static-field collection. Operation conditions for spectral acquisition: microwave frequency, 9.37 GHz; modulation frequency, 100 kHz, modulation amplitude, 2.0 G_{pp}; receiver gain, 2×10^5.

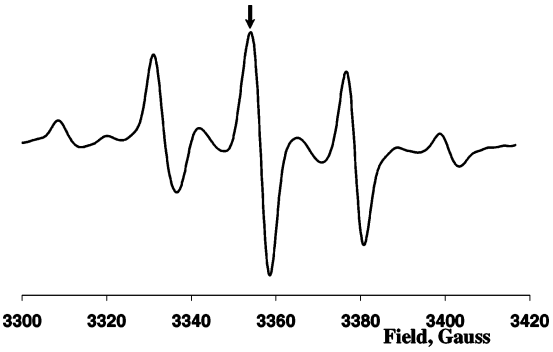

Figure 6. Typical 9-line methacrylate-propagating radical EPR spectra acquired during the polymerization of TEGDMA. Arrow indicates the field position used during static-field-collection. Operation conditions for spectral acquisition: microwave frequency, 9.42 GHz; modulation frequency, 100 kHz; modulation amplitude, 2.0 G_{pp}; receiver gain, 4×10^4.

environment (Figure 5) is observed throughout the polymerization. At long irradiation times, well after essentially complete conversion of the double bonds is achieved, evidence of an overlapping 9-line species is visible. The 9-line spectrum is typically associated with the propagating radical in a more mobility-restricted environment. Thus, the absence of a transition to the 9-line in the PEG(600)DMA system is evidence of a relatively high mobility polymerization environment. Unlike the PEG(600) system, TEGDMA does not remain above its glass transition temperature throughout the entirety of the polymerization. The difference in the two system's polymerization environments is manifested in the observed spectra. At the conditions examined here, the 13-line spectrum is never observed in the TEGDMA polymerization. The polymerization environment is such that only the 9-lines species (Figure 6) is visible once the radical population reaches the spectrometer's detection limit, $\sim 10^{-6}$ mol/L. It should be noted that a transition from the 13-line to the 9-line is visible in many materials, and thus multiple conversion dependent peak height to spectrum area calibrations may be necessary to capture the polymerization characteristics accurately in those systems.

Spectral changes are not observed with the static-field-collection method, but when used in conjunction with full spectral acquisitions, a great deal of information is obtained. Millisecond resolutions are possible using the static-field technique. Plots of radical profiles for the photopolymerization of PEG(600)DMA using the two data acquisition techniques are presented in Figure 7. The solid lines represent static-field acquisition, and the points represent full-spectrum acquisitions. The amount of information lost as a result of the long times required to obtain complete spectra is apparent when comparing the two techniques (—, static field; ○, full spectrum). A rapid increase in the radical concentration at the

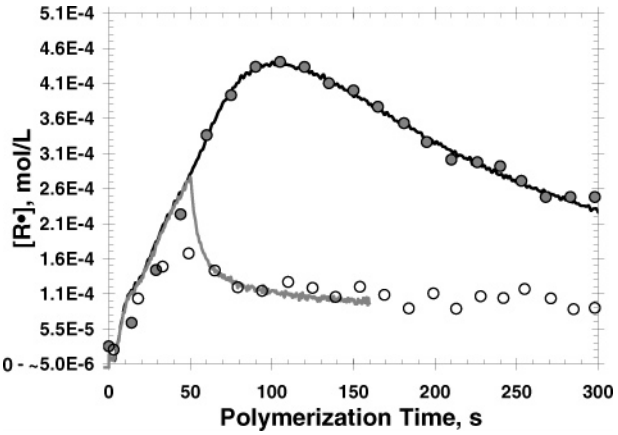

Figure 7. A comparison of static-field (black line, gray line) and full spectrum acquisition techniques (●, ○) for obtaining radical concentration profiles for the polymerization of PEG-(600)DMA. Note that the short time scale features of the radical population evolution and decay are not captured by the full spectrum data. Irradiation times are 50 (○) and 300 (●) seconds at 5 mW/cm^2. The static-field plots were acquired at resolutions of 20 and 40 ms/datapoint for the 50- and 300-s cure times, respectively.

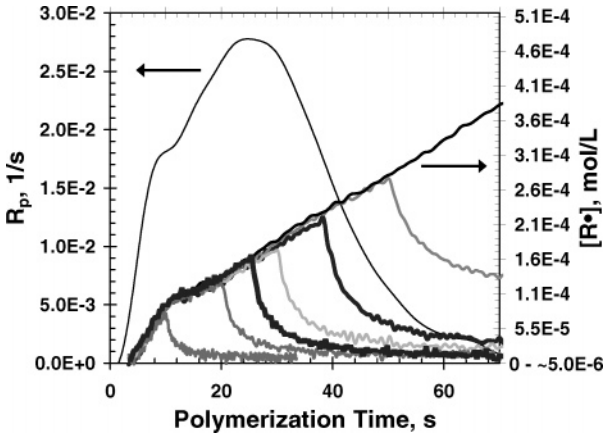

Figure 8. Polymerization rate (left axis) and radical concentration profiles (right axis) as a function of irradiation time. The rate curve was obtained using the derivative of the NIR−FTIR conversion vs time data with irradiation for 300 s. This plot illustrates both full-cure and partial-cure results for the polymerization of PEG(600)DMA initiated with 0.1 wt % DMPA and 5mW/cm^2 of UV light using EPR spectroscopy.

onset of polymerization is clearly visible in the static-field collection results. This initial increase is followed by another region of radical generation with a slower rate. The analysis of the full-spectrum data does not exhibit these two distinct regions of radical generation. The details of the initial increase and the transition to a second region of slower radical generation are lost in the time-averaged full-spectrum collection method. Similarly, the close adherence to the full cure data and then the rapid decay in the absence of initiation are also not observed in the full-spectrum data. The clearly resolved behavior of the static-field result is reduced to a single time-averaged point that does not provide an accurate depiction of the true rate behavior in that region. This time-averaged nature of the full spectrum data makes quantification of the termination kinetic constant immediately after the light is extinguished nearly impossible.

EPR Analysis. This experimental procedure is used to obtain individual rate constants, k_p and k_t, as a function of conversion in the absence of the underlying assumptions necessary to gather this information using techniques such as FTIR and DSC. A comparison between the data obtained with EPR and that which has been obtained with other techniques is also utilized to understand the polymerization kinetics better by quantifying the fraction of radicals that actually participate in the propagation reaction as a function of monomer conversion.

Termination Kinetic Constant Evaluation. The change in the radical concentration with time during the polymerization is represented by eq 7 where R_i is the initiation rate and a bimolecular, chain length independent termination mechanism is assumed

$$\frac{d[\mathrm{R}\bullet]}{dt} = R_i - 2k_t[\mathrm{R}\bullet]^2 \tag{7}$$

The decay of the radical concentration in the absence of the initiation reaction (i.e., when $R_i = 0$) is then directly related to the termination behavior of the system via eq 8, where $[\mathrm{R}\bullet]_0$ is the radical concentration at the time that the light was extinguished, or any time zero in the dark, and $[\mathrm{R}\bullet]_t$ represents the radical concentration at time t since the light was extinguished

$$\frac{[\mathrm{R}\bullet]_0}{[\mathrm{R}\bullet]_t} = 1 + 2k_t[\mathrm{R}\bullet]_0 t \tag{8}$$

Polymerizations are monitored with different irradiation times, and radical concentration profiles are obtained for the system both during irradiation and post irradiation (Figure 8). The postirradiation plots of $[\mathrm{R}\bullet]_0/[\mathrm{R}\bullet]_t$ vs time in the absence of initiation are then used to examine the termination kinetics of each system (eq 8). Parallel NIR−FTIR experiments facilitate correlation of kinetic parameters with double bond conversion.

Propagation Kinetic Constant Evaluation. The propagation kinetic constant, k_p, is obtained by combining the NIR−FTIR and EPR techniques. Polymerization rate and double-bond conversion as a function of polymerization time are directly obtained from NIR. Radical concentration as a function of polymerization time is obtained from EPR evaluation of the same system at the same conditions. Knowing the relationship between polymerization rate, R_p, and the reactant concentration, i.e., double bonds, [M], and radicals, [R•], k_p is calculated (eq 9)

$$R_p = k_p[\mathrm{M}][\mathrm{R}\bullet] \tag{9}$$

Thus, only a single steady-state polymerization experiment from each technique, combining both the EPR and the NIR−FTIR, is necessary to obtain k_p as a function of conversion for the entire polymerization. This measure of k_p is then compared with that obtained from NIR−FTIR alone.

"Active" Radical Kinetic Constant Evaluation. Kinetic parameters that account for the persistent radical concentration present in the polymer network are also available with EPR. The radical concentration does not decay completely, i.e., to undetectable levels, after irradiation cessation in each unsteady-state experiment. This result implies that a percentage of the radical population is not participating in termination reactions on the time scale of the unsteady-state experiment (5−10 min on average). Removal of the persistent radical population concentration, $[\mathrm{R}\bullet]_{\mathrm{persistent}}$, from the total radical population, $[\mathrm{R}\bullet]_{\mathrm{total}}$, facilitates "active" radical kinetic constant determination. Thus, eq 10 is substituted into eqs 8 and 9 and $k_{t,\mathrm{active}}$ and $k_{p,\mathrm{active}}$ are calculated. The persistent radical concentration is quantified as the plateau radical concentration taken ~10 min after extinction of the irradiation source

$$[\mathrm{R}\bullet] = [\mathrm{R}\bullet]_{\mathrm{total}} - [\mathrm{R}\bullet]_{\mathrm{persistent}} \tag{10}$$

Results and Discussion

FTIR and EPR were used to obtain rate data and kinetic parameters for the polymerization of both a rubbery and a glassy polymer forming dimethacrylate.

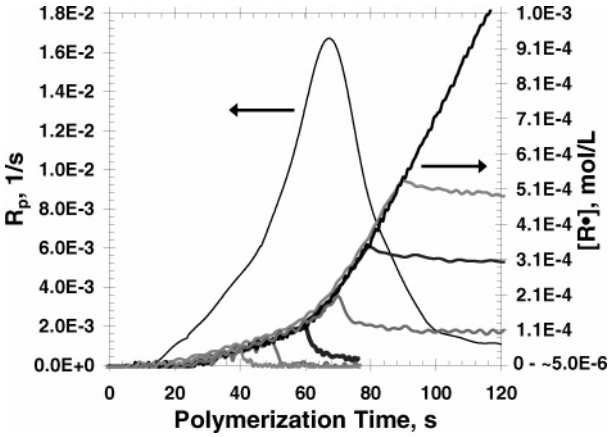

Figure 9. TEGDMA polymerization rate (left axis) and radical concentration profiles (right axis) as a function of irradiation time. The rate curve was obtained using the derivative of the NIR−FTIR conversion vs time data with irradiation for 300 s. This plot illustrates both full-cure and partial-cure results for the polymerization of TEGDMA initiated with 0.1 wt % DMPA and 5mW/cm^2 of UV light using EPR spectroscopy.

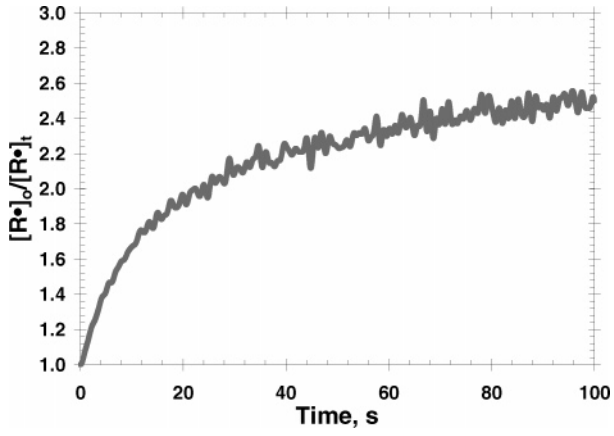

Figure 10. PEG(600)DMA "in the dark" termination kinetic constant evaluation from a plot of the initial "dark" radical concentration, $[R•]_0$, divided by the "dark" radical concentration as a function of time, $[R•]_t$. Polymerization conditions: temperature, 25 °C; light intensity during polymerization, 5 mW/cm^2; initiator concentration, 0.1 wt % DMPA; duration of irradiation, 50 s. EPR operation conditions: microwave frequency, 9.37 GHz; modulation frequency, 100 kHz; modulation amplitude, 2.0 G_{pp}; gain, 2×10^5.

A rapid increase in the radical concentration at the onset of polymerization is observed in the rubbery PEG(600)DMA system (Figure 8). The radical population evolution rate then slows to a second approximately constant value until the polymerization is complete with respect to the decay of double bonds in the system. This transition appears to occur simultaneously with the onset of autoacceleration. This result is somewhat unexpected, as the onset of autoacceleration is typically thought to be accompanied by a dramatic increase in radical concentration, induced by ever-increasing mobility limitations to termination.

The glassy TEGDMA polymerization system also exhibits a transition in the rate of change of the radical concentration (Figure 9). The transition appears somewhat delayed in relation to what was observed in the PEG(600) system, and the trend is reversed, i.e., an increase in the [R•] vs time slope is observed. This result is more intuitive with respect to the nature of autoacceleration in cross-linking polymerizations. It is also worth noting that a transition in the unsteady-state behavior also seems to occur at this point, namely, a transition from a radical population that almost entirely decays in the absence of initiation to one that includes a significant radical concentration that persist long after the initiating light source has been extinguished.

Figure 10 illustrates the termination analysis for PEG(600)DMA. Several different regions of termination are observed. The presence of more than one termination regime is typical of all of the multivinyl systems that we have studied. Similar behavior was also observed by Buback et al. in their EPR evaluation of the low conversion (<30%) termination kinetics of dodecyl methacrylate (DMA).[5] A possible explanation for the different termination regions involves the presence of different time scales for termination of radicals of different lengths, i.e., chain-length-dependent termination (CLDT). This explanation was also hypothesized for the linearly polymerizing DMA.[5] The concept of CLDT, while broadly accepted in linearly polymerizing systems, has been explored only recently in multivinyl polymerizations.[47−50] In this scenario, one might envision a partially formed network (Figure 11a) that contains several different reactive species. At any given

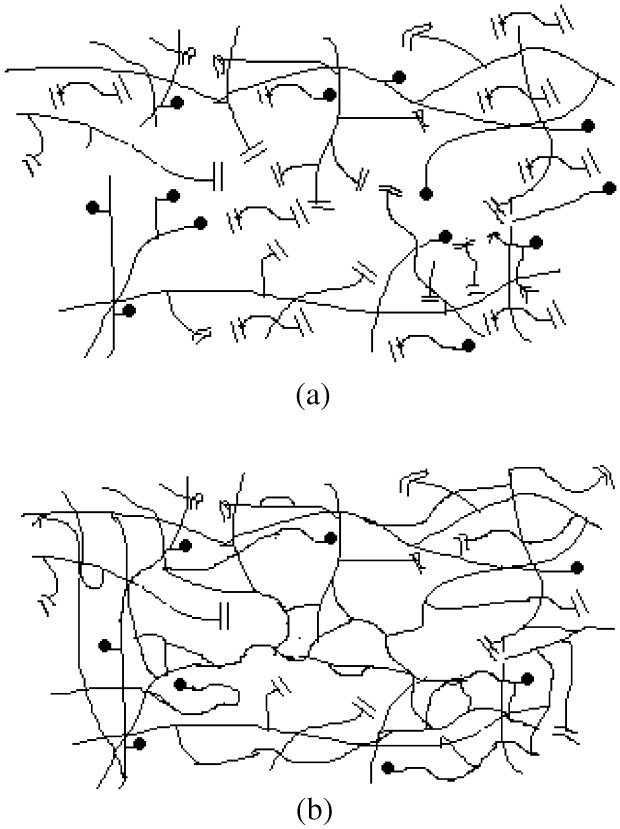

Figure 11. (a) An example network structure at the time that the light is extinguished. Radicals can encounter each other via center-of-mass diffusion, segmental motion, and reaction diffusion during this time. (b) The network structure from (a) some time after the light was extinguished and after the more mobile radical species have been consumed. It is more difficult for the radicals to encounter one another at this point in time.

time during polymerization, unreacted monomer, low molecular weight (MW) radicals up to some MW < MW_c, a critical MW after which the radical behaves as a "long" radical, and "long" radicals and double bonds with significant mobility only beyond their last tether point to the network are present in the system. If this network

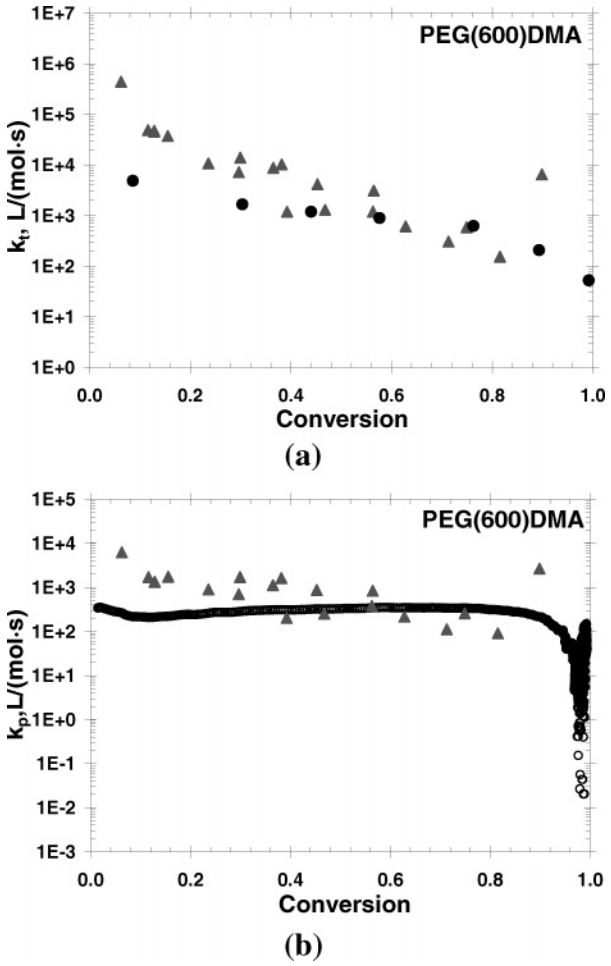

Figure 12. (a) Termination kinetic constant, $k_{t,mobile}$, and (b) propagation kinetic constant, k_p, for the photopolymerization of PEG(600)DMA as obtained from FT-NIR analysis (▲) and EPR analysis (●). Polymerization conditions: light intensity, 5 mW/cm^2; initiator concentration, 0.1 wt %.

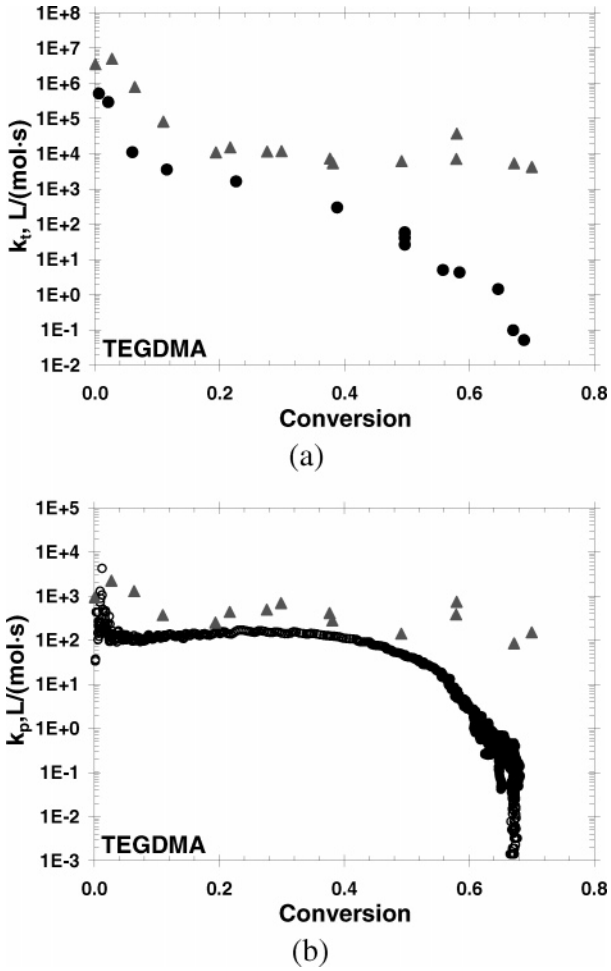

Figure 13. (a) Termination kinetic constant, $k_{t,mobile}$, and (b) propagation kinetic constant, k_p, for the photopolymerization of TEGDMA as obtained from FT-NIR analysis (▲) and EPR analysis (●). Polymerization conditions: light intensity, 5 mW/cm^2; initiator concentration, 0.1 wt %.

exists at the time that the light is extinguished, then the smaller and more mobile radicals and double bonds will react and terminate during the first region of termination, immediately after the light is extinguished. After some period of time in the absence of the initiation reaction, one hypothesis is that all of the more mobile species have reacted and the network has become more cross linked (Figure 11b). Thus, a continuous change in the average k_t, represented by the continuously changing slope of the data presented in Figure 10, is observed. The duration of this initial period is likely controlled by a number of network properties: primarily a combination of the chemical reactivity and the effective diffusion coefficients of the more mobile radical species in the network and correspondingly, the maximum size of a chain before it is too large to be considered mobile relative to the network characteristics. Following the initial period of rapid termination, the remaining reactive species will continue to find each other and terminate but over much longer time scales, since the smaller, more mobile radical population has been depleted. Now, radicals are either separated by large distances or are tethered closely to the network, lowering the probability of encountering another radical at each time step.

The radical concentration profiles from the full and unsteady-state experiments using static-field EPR, Figures 8 and 9, were used to obtain $k_{t,mobile}$ or the short time termination kinetic constant as a function of conversion for both polymerization systems. The termination kinetic constants for PEG(600)DMA and TEGDMA obtained from two techniques, FTIR and EPR, have been compared in Figures 12a and 13a. Termination kinetic parameters collected with these two techniques for the polymerization of PEG(600)DMA exhibited good agreement despite the assumptions necessary to analyze the FTIR data. The measurement of k_t at higher conversion values is easily obtained using EPR, whereas this measurement becomes difficult using FTIR because small errors in the measurement of conversion have a large impact on the resulting k_t. This difficulty is accentuated with a monomer such as PEG(600)DMA that reaches complete conversion. In contrast, the termination kinetics of the TEGDMA polymerization acquired using the two different analytical techniques exhibit significant differences throughout the polymerization, with the EPR data exhibiting consistently lower k_t values than those measured using FTIR.

Propagation kinetic parameters are also obtained from EPR analysis in conjunction with rate data, in this case as determined from NIR−FTIR spectroscopy. This measure of k_p is then compared with that obtained from NIR−FTIR alone. These results for the polymerization of PEG(600)DMA and TEGDMA are presented in Figures 12b and 13b, respectively. Again, better agreement is observed in the rubbery PEG(600)DMA polymeriza-

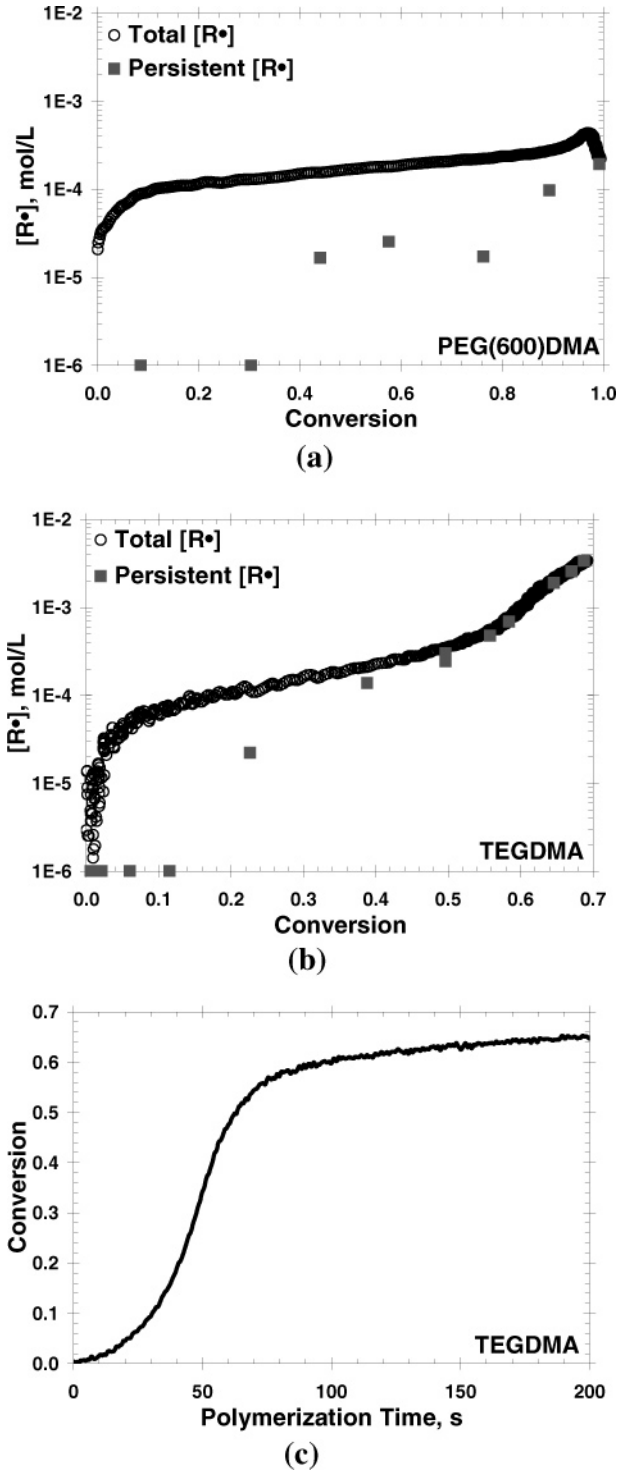

Figure 14. The persistent radical population (■) compared with the total radical population (○) as a function of conversion for (a) PEG(600)DMA and (b) TEGDMA polymerization and (c) the corresponding conversion vs time information for TEGDMA. Polymerization conditions: light intensity, 5 mW/cm^2; initiator concentration, 0.1 wt %.

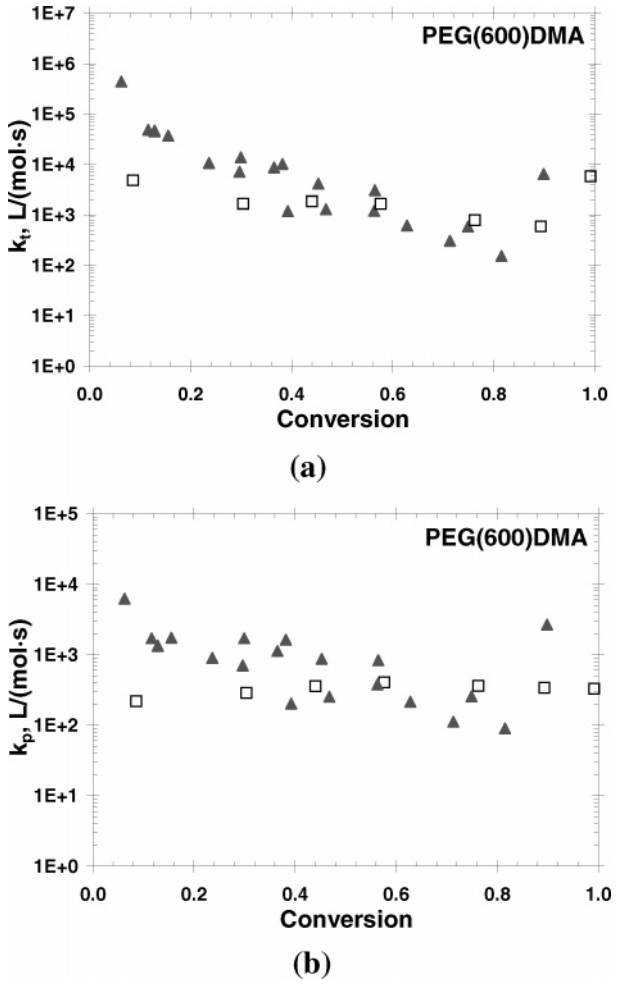

Figure 15. A comparison of the (a) termination kinetic constant, k_t, and (b) propagation kinetic constant, k_p, for photopolymerization of PEG(600)DMA as obtained from FT-NIR analysis (▲) and EPR analysis of the "active" radical population (□). Polymerization conditions: light intensity, 5 mW/cm^2; initiator concentration, 0.1 wt %.

tion system. One explanation for the deviations realized in the TEGDMA polymerization system involves the presence of a significant persistent radical population during the polymerization; thus, implying that a fraction of the radical population does not readily participate in termination and/or propagation reactions. This result leads to a different measure of the kinetic constants when examining the change in radical concentration, EPR, as opposed to the double-bond concentration, FTIR. The contribution of this effect to the kinetic parameters is quantified by measuring the persistent radical populations and excluding them from the measure of k_t and k_p, in essence using only the "active" radical concentration for those calculations.

Persistent Radical Populations. The quantification of the persistent radical populations that remain post polymerization is of interest for other reasons as well. Of primary interest industrially is the impact that this radical population has on the long-term material properties of a polymer product. It has been hypothesized that the presence of a persistent radical population within a polymer network post cure leads to property deterioration over time due to the formation of peroxy radicals via reaction with atmospheric oxygen. Additionally, these radicals that remain in the system after cure facilitate further reaction when the polymer is exposed to environmental changes such as thermal cycling. Such reactions also significantly affect the material properties. The quantity of persistent radicals is highly dependent on the nature of the polymer network that is formed and on the duration of sample irradiation.

These persistent radical populations have been quantified and compared with the total radical population as a function of conversion for both PEG(600)DMA and

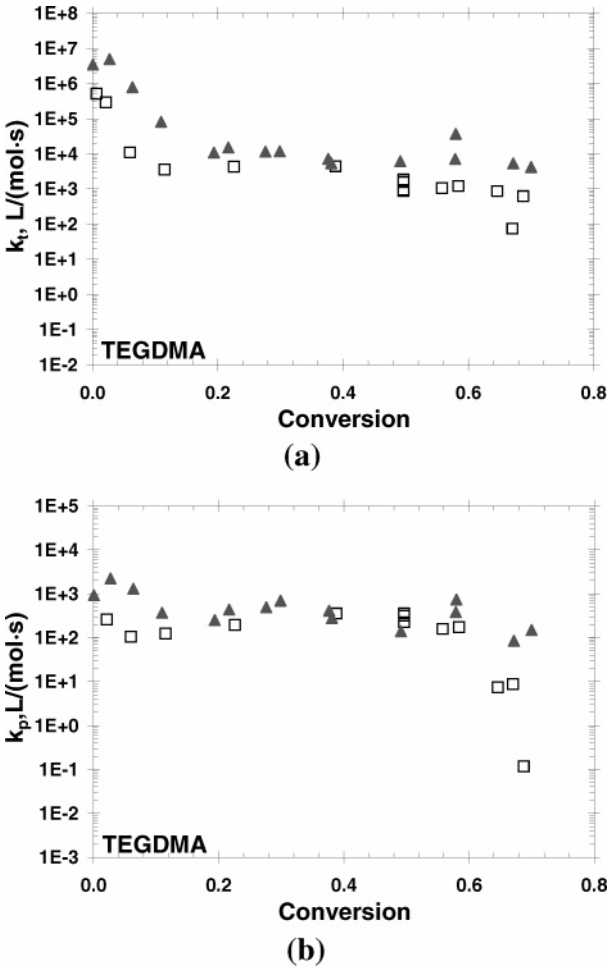

Figure 16. A comparison of the (a) termination kinetic constant, k_t, and (b) propagation kinetic constant, k_p, for photopolymerization of TEGDMA as obtained from FT-NIR analysis (▲) and EPR analysis of the "active" radical population (□). Polymerization conditions: light intensity, 5 mW/cm^2; initiator concentration, 0.1 wt %.

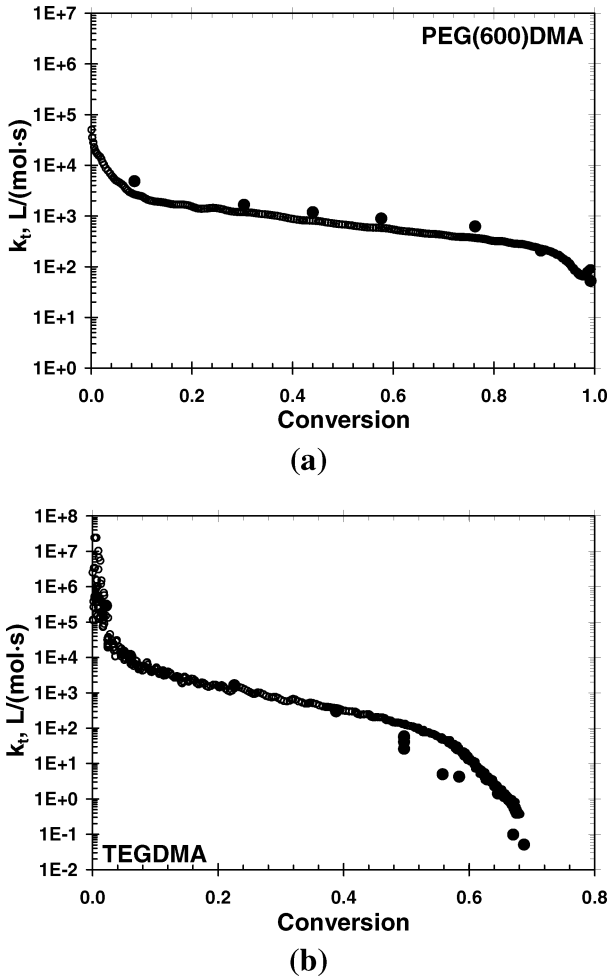

Figure 17. A comparison of the termination kinetic constant, k_t, as determined from EPR evaluation of the total radical population (●) and from the pseudo-steady-state assumption (○) assuming an initiator efficiency of unity for the polymerization of PEG(600)DMA and TEGDMA. Polymerization conditions: light intensity, 5 mW/cm^2; initiator concentration, 0.1 wt %.

TEGDMA (Figure 14). Conversion vs time behavior for the polymerization of PEG(600)DMA and TEGDMA has also been presented in Figures 2a and 14c, respectively, to facilitate comparisons between all presented data. Not surprisingly, the rubbery PEG(600)DMA network does not possess a significant persistent radical population until about 40% conversion. In contrast, the glassy TEGDMA network contains a stable radical population by 20% conversion. These conversions are consistent with when each system's termination behavior becomes reaction diffusion controlled.

These measures of persistent radical populations are subsequently used in the analysis of the termination and propagation kinetic constants to obtain a measure of those parameters as they pertain to the "active" radical population. Those results are presented in Figures 15 and 16 for the polymerizations of PEG(600)-DMA and TEGDMA, respectively. Accounting for this "unreactive" population, as expected, has a minimal effect on the PEG(600)DMA kinetics. However, accounting for this population in the glassy TEGDMA system transforms results that were in very poor agreement into ones that are much closer quantitatively. This analysis demonstrates the importance of accounting for persistent radical populations if the goal is to characterize the kinetics of the most mobile of the radical species. Correspondingly, such analyses also provide insight into the role of persistent radial populations in dictating the overall polymerization kinetics as a function of the characteristics of the network formed.

Pseudo-Steady-State Assumption. Evaluating the validity of the pseudo-steady assumption to calculate k_t as a function of conversion for the total radical population was also of interest. Thus, eq 11 was used to calculate k_t from a single steady-state polymerization run in the cavity of an EPR spectrometer and an assumed knowledge of the initiation rate, R_i. An efficiency of 1 was used for these calculations, and the results are presented in Figure 17.

Interestingly the results obtained from this single experiment are in very close agreement with those obtained after the painstaking analysis of numerous unsteady-state runs! It is important to point out that no information about the persistent radical populations is available from the steady-state experiment, and thus the total radical population, $[R\bullet]_{total}$, was used in eq 11 instead of the more accurate $[R\bullet]_{active}$, as the persistent population by definition does not participate in bimolecular termination reactions. However, analysis of unsteady-state experiments purely for the persistent radical populations as a function of conversion would allow for their application to these results.

Conclusions

The combination of EPR with FT-NIR provides a comprehensive picture of radical population characteristics during polymerization as well as information that is otherwise unavailable to these techniques individually. Evaluation of two multimethacrylate polymerization systems, one forming a rubbery polymer network and the other a glassy network, revealed numerous differences in their polymerization attributes as characterized by this experimental technique combination. Specifically, their steady-state radical concentration profiles, the environment of their propagating radicals throughout the majority of the polymerization, and the differences in their termination and propagation kinetics as a function of total and persistent radical concentrations were in stark contrast. Kinetic parameters obtained with EPR were also compared with those obtained independently from the FT-NIR technique. The FT-NIR-obtained kinetic constants are in good agreement with the "active" radical kinetic constants obtained from the EPR/FT-NIR combination. The results of these studies illustrate that EPR is a powerful technique that is readily applicable to kinetic evaluation of free radical photopolymerizations. The application of EPR provides insight into the complex polymerization kinetics and corresponding network formation, and as a result, a more complete understanding of the anomalous behaviors exhibited by these polymerizations is attained.

Acknowledgment. The authors thank J.W. Stansbury for preparation of the hydrogenated monomers and Marc Desrosiers, NIST, for his helpful discussions regarding EPR. The authors also thank the IUCRC for Fundamentals and Applications of Photopolymerizations and the National Institute of Health (NIH Grant DE 10959) for research funding, the Department of Education for granting GAANN doctoral fellowships to K.A.B., and the LANL LDRD Postdoctoral Fellows Program for granting a fellowship to K.A.B. Los Alamos National Laboratory is operated by the University of California for the United States DOE under Contract W-7405-ENG-36.

References and Notes

(1) Ranby, B.; Rabek, J. F. *ESR Spectroscopy in Polymer Research*; Springer: Berlin, 1977.
(2) Kamachi, M. *Adv. Polym. Sci.* **1987**, *82*, 207−275.
(3) Yamada, B.; Westmoreland, D. G.; Kobatake, S.; Konosu, O. *Prog. Polym. Sci.* **1999**, *24*, 565−630.
(4) Zetterlund, P. B.; Yamauchi, S.; Yamada, B. *Macromol. Chem. Phys.* **2004**, *205*, 785.
(5) Buback, M.; Egorov, M.; Junkers, T.; Panchenko, E. *Macromol. Rapid Commun.* **2004**, *25*, 1004−1009.
(6) Zetterlund, P. B.; Yamazoe, H.; Yamauchi, S.; Yamada, B. *ACS Symp. Ser.* **2003**, *854*, 85.
(7) Le, T. T.; Hill, D. J. T. *Polym. Int.* **2003**, *52*, 1700.
(8) Zetterlund, P. B.; Yamada, B. *Abstr. Pap. Am. Chem. Soc.* **2002**, *224*, U481.
(9) Zetterlund, P. B.; Yamazoe, H.; Yamada, B.; Hill, D. J. T.; Pomery, P. J. *Macromolecules* **2001**, *34*, 7686−7691.
(10) Yamazoe, H.; Zetterlund, P. B.; Yamada, B.; Hill, D. J. T.; Pomery, P. J. *Macromol. Chem. Phys.* **2001**, *202*, 829.
(11) Yamada, B.; Azukizawa, M.; Yamazoe, H.; Hill, D. J. T.; Pomery, P. J. *Polymer* **2000**, *41*, 5611−5618.
(12) Azukizawa, M.; Yamada, B.; Hill, D. J. T.; Pomery, P. J. *Macromol. Chem. Phys.* **2000**, *201*, 774−781.
(13) Kajiwara, A.; Kamachi, M. *Macromol. Chem. Phys.* **2000**, *201*, 2165−2169.
(14) Kamachi, M.; Kajiwara, A. *Macromol. Chem. Phys.* **2000**, *201*, 2160−2164.
(15) Seno, M.; Fukui, T.; Hirano, T.; Sato, T. *J. Polym. Sci., Part A: Polym. Chem.* **2000**, *38*, 4264−4271.
(16) Garcia, N.; Guzman, J.; Riande, E.; Calle, P.; Sieiro, C. *Polymer* **2001**, *42*, 6425−6430.
(17) Anseth, K. S.; Anderson, K. J.; Bowman, C. N. *Macromol. Chem. Phys.* **1996**, *197*, 833−848.
(18) Berchtold, K. A.; Randolph, T. W.; Bowman, C. N. *Polym. Mater. Sci. Eng.* **2003**, *88*, 213-214.
(19) Lovell, L. G.; Berchtold, K. A.; Elliott, J. E.; Lu, H.; Bowman, C. N. *Polym. Adv. Technol.* **2001**, *12*, 335−345.
(20) Zhu, S.; Tian, Y.; Hamielec, A. E.; Eaton, D. R. *Polymer* **1990**, *31*, 154−159.
(21) Sakai, Y.; Iwasaki, M., *J. Polym. Sci., Part A: Polym. Chem.* **1969**, *7*, 1749−1764.
(22) Iwasaki, M.; Sakai, Y. *J. Polym. Sci., Part A: Polym. Chem.* **1969**, *7*, 1537−1547.
(23) Sakai, Y.; Iwasaki, M. *J. Polym. Sci., Part A: Polym. Chem.* **1969**, *7*, 3143−3150.
(24) Best, M. E.; Kasai, P. H. *Macromolecules* **1989**, *22*, 2622.
(25) Tian, Y.; Zhu, S.; Hamielec, A. E.; Fulton, D. B.; Eaton, D. R. *Polymer* **1992**, *33*, 384−390.
(26) Doetschman, D. C.; Mehlenbacher, R. C.; Cywar, D. *Macromolecules* **1996**, *29*, 1807−1816.
(27) Selli, E.; Oliva, C.; Termignone, G. *J. Chem. Soc., Faraday Trans.* **1994**, *90*, 1967−1972.
(28) Placek, J.; Szocs, F. *Eur. Polym. J.* **1989**, *25*, 1149−1152.
(29) Szocs, F.; Lazar, M. *Eur. Polym. J.* **1969**, *(Suppl.)*, 337.
(30) Oliva, C.; Selli, E.; Diblas, S.; Termignone, G. *J. Chem. Soc., Perkin Trans. 2* **1995**, 2133-2139.
(31) Matsumoto, A.; Giese, B. *Macromolecules* **1996**, *29*, 3758−3772.
(32) Zhu, S.; Tian, Y.; Hamielec, A. E.; Eaton, D. R. *Polymer* **1990**, *31*, 1726−1734.
(33) Fitzwater, S.; Chang, H. R.; Parker, H. Y.; Westmoreland, D. G. *Macromolecules* **1999**, *32*, 3183−3189.
(34) Parker, H. Y.; Westmoreland, D. G.; Chang, H. R. *Macromolecules* **1996**, *29*, 5127.
(35) Kloosterboer, J. G.; Hei, G. M. M. V. d.; Gossink, R. G.; Dortant, G. C. M. *Polymer Commun.* **1984**, *25*, 322.
(36) Kloosterboer, J. G.; Lijten, G. F. C. M.; Greidanus, F. J. A. M. *Polymer Commun.* **1986**, *27*, 268−271.
(37) Fraenkel, G. K.; Hirshon, J. M.; Walling, C. *J. Am. Chem. Soc.* **1954**, *76*, 3606.
(38) Decker, C.; Moussa, K. *J. Polym. Sci., Part A: Polym. Chem.* **1987**, *25*, 739−742.
(39) Selli, E.; Oliva, C.; Galbiati, M.; Bellobono, I. R. *J. Chem. Soc., Perkin Trans. 2* **1992**, *9*, 1391−1395.
(40) Selli, E.; Oliva, C.; Giussani, A. *J. Chem. Soc., Faraday Trans.* **1993**, *89*, 4215−4219.
(41) Rueggeberg, F. A.; Hashinger, D. T.; Fairhurst, C. W. *Dent. Mater.* **1990**, *6*, 241−249.
(42) Lovell, L. G.; Stansbury, J. W.; Syrpes, D. C.; Bowman, C. N. *Macromolecules* **1999**, *32*, 3913−3921.
(43) Berchtold, K. A.; Bowman, C. N. *RadTech Europe '99*; Berlin, Germany, 1999; p 767.
(44) Anseth, K. S.; Decker, C.; Bowman, C. N. *Macromolecules* **1995**, *28*, 4040−4043.
(45) Odian, G. *Principles of Polymerization*, 3rd ed.; John Wiley & Sons: New York, 1991.
(46) Wertz, J. E.; Bolton, J. R. *Electron Spin Resonance: Elementary Theory and Practical Applications*; McGraw-Hill: New York, 1972.
(47) Berchtold, K.; Lovestead, T.; Bowman, C. *Macromolecules* **2002**, *35*, 7968−7975.
(48) Berchtold, K. A.; Hacioglu, B.; Lovell, L. G.; Nie, J.; Bowman, C. N. *Macromolecules* **2001**, *34*, 5103−5111.
(49) Berchtold, K. A.; Lovell, L. G.; Nie, J.; Hacioglu, B.; Bowman, C. N. *Polymer* **2001**, *42*, 4925−4929.
(50) Lovestead, T.; Berchtold, K.; Bowman, C. *Macromol. Theory Simul.* **2002**, *11*, 729−738.

MA0506482